

Lattice Boltzmann Simulations of Flow Past a Cylindrical Obstacle

Lukas Wagner¹ and Fernand Hayot¹

Received September 9, 1994; final February 1, 1995

We present lattice Boltzmann simulations of flow past a cylindrical obstacle. Our study is based on the Lévy walk model of turbulence in a lattice Boltzmann model. We discuss pressure around the cylinder with laminar and “turbulent” incident flows, as well as the dependence of the von Karman street on the analog of integral scale in our model.

KEY WORDS: Turbulence modeling; lattice Boltzmann methods; wakes.

The lattice Boltzmann (LB) scheme of Chen *et al.*⁽¹⁾ provides a simple numerical scheme for the description of fluid flow. We use this LB scheme to investigate laminar flow around a cylinder⁽²⁾ and also as a basis for modeling the effect of turbulence in the incident flow. Needless to say, these results are obtained within the model we are considering, and are only suggestive. They are meant to elicit experimental⁽³⁾ and other theoretical work on the subject of turbulent scales and coherent structures.

We mimic momentum transport by an eddy of size l by exchanging the populations of two randomly chosen sites separated by l , with l chosen with a probability $p(l) \propto l^{-1.3}$ for all results presented here. In agreement with the discussion of Schlesinger *et al.*,⁽⁴⁾ we associate a waiting time with each length l . Since the waiting time is the reciprocal of the frequency of jumps of a particular length, the distribution of waiting times is set by the dependence of the number of exchanges $N(l)$ on l . We use here $N(l) \propto N_0 - l$.

We implement this model in two-dimensional flow past a circular obstacle. The obstacle is set into a channel with uniform velocity U at the boundaries in the streamwise direction x and periodic boundaries in the

¹ Department of Physics, Ohio State University, Columbus, Ohio 43210.

transverse y direction, with origin at the center of the obstacle. A more precise description of the flow geometry may be found elsewhere.⁽²⁾ This is an extension of our previous study of a Lévy walk-based model of turbulence in a Boolean implementation of channel flow.⁽⁵⁾ Here, in addition to being able to resolve more precisely the velocity field, we are able to investigate pressure because of the absence of statistical noise characteristic of Boolean approaches.

There are two basic length scales when the LB model with exchanges is used to model cylinder flow with incident turbulence. One is l_{\max} , the maximum allowed exchange length, which sets a length scale for the turbulent exchanges. In our model l_{\max} plays the role of the integral scale in experimental studies. The second length scale in flow past an obstacle is just the obstacle diameter D . It is the ratio of these two length scales, which is the crucial parameter for investigating the impact of turbulence in flow impinging on a cylinder.

One difficulty in finding pressure at a surface in the LB method not present with finite-difference methods is that a perfectly circular obstacle cannot be created on a regular lattice with no-slip boundary conditions. The edges of an approximation to a circle on a lattice are jagged, which produces discernible effects in the flow very near the obstacle. Evaluating the pressure at the surface of the obstacle does not yield a smooth $p(\theta)$. This is a difficulty which cannot be resolved by interpolating, but is due to the perturbation of the flow by a polygonal obstacle. It is necessary to evaluate the pressure several sites (roughly a mean free path) away from the surface of the obstacle to obtain a curve that does not show discontinuities due to the lattice. Doing so introduces appreciable error both at the leading edge of the obstacle and at the angle of minimum pressure.⁽²⁾ Results presented in the inset to Fig. 6 are thus for pressure evaluated four lattice sites away from the surface of the obstacle.

The pressure in *laminar* flow as calculated in the LB scheme without exchanges agrees with experimental^(6, 7) and finite-difference studies.^(8, 9) A succinct measure of the accuracy of our laminar solution is the Strouhal number $St = D/\tau U$, where τ is the period of the oscillation in drag, or, equivalently, in $v(x, 0)$; we find $St = 0.162$, as compared to $St = 0.153$ for the experimental results,⁽⁷⁾ an error of 6%. This figure may be compared with errors for St of $\leq 3.5\%$ in the exacting numerical study of Abarbanel *et al.*⁽⁹⁾

Figures 1 and 2 show the pressure field without and with exchanges, respectively, at a mean-flow Re of 76.8. The symmetric pressure field shown in Fig. 3 suggests that in this case the von Karman street is destroyed by incident turbulence. This is easily verified by inspecting the dependence of $v(3.5D, 0)$, the component of the velocity perpendicular to the mean flow

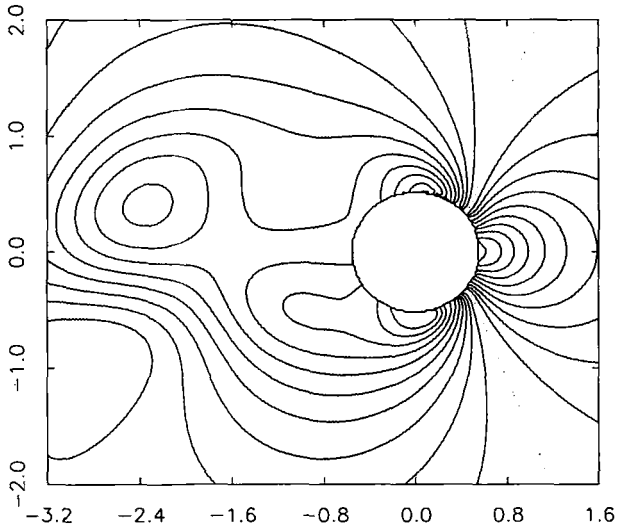


Fig. 1. Contour plot of dimensionless pressure at $Re=76.8$. Dotted line is $p = p_{inf}$, with each contour representing a step of $0.1p'$.

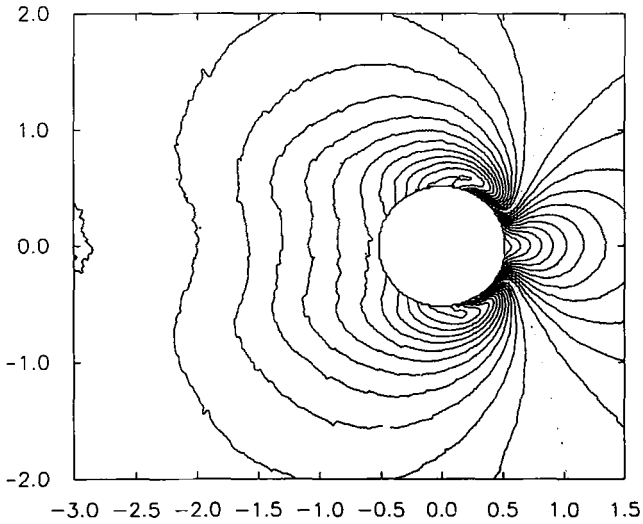


Fig. 2. Contour plot of dimensionless pressure at $Re=76.8$ with Lévy model of incident turbulence; $l_M = 7D$, contour lines defined as for Fig. 2.

at a position 3.5 diameters downstream of the obstacle's center, on l_{\max} , which is shown in Fig. 3. The inset shows how the time series of $v(3.5D, 0)$ changes character with increasing exchange length; the intermittent intervals of regular oscillation in the velocity become rarer with increasing exchange length.

An examination of u , the streamwise velocity, suggests a simple explanation for why the exchanges suppress the von Karman street. The wake length L is the distance upstream from the obstacle center where u at $y=0$ becomes positive. The wake behind the obstacle is much shorter with incident turbulence as modeled by Levy distributed exchanges ($L=1.1D$) than without ($L=2.6D$). Both the shortened wake and the absence of vortex shedding are explained by the effect of the enhanced momentum transport provided by the Lévy distributed exchanges. The exchanges (and the eddies which they model) transport momentum between the slowly moving fluid behind the obstacle and the fast-moving fluid to either side. The net effect is to accelerate the fluid behind the obstacle, thus shortening the wake. The same mechanism of enhanced momentum transport affects the region immediately behind the obstacle, where vortices form before

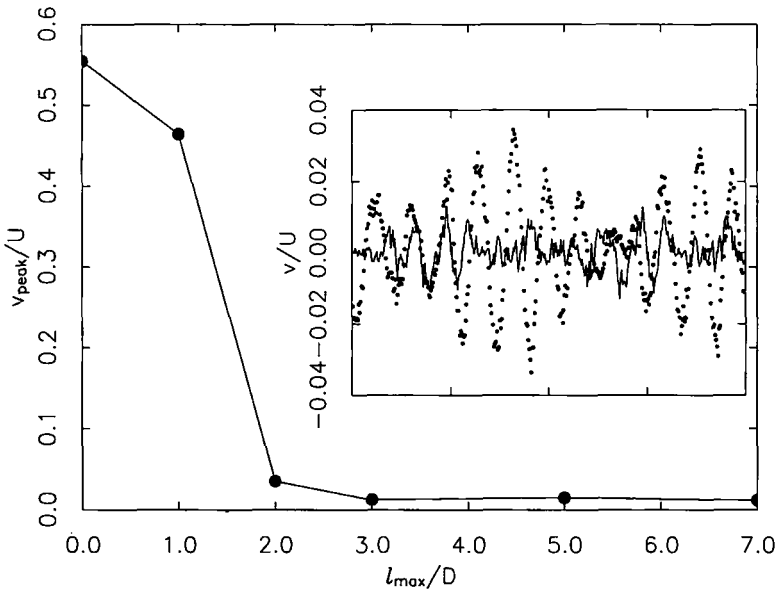


Fig. 3. Peak transverse velocity measured at a station 3.5 diameters downstream from the obstacle center, $v(3.5D, 0)$, plotted against maximum exchange length. Inset shows time series of $v(3.5D, 0)$ for $l_{\max} = 2D$ (dots) and $3D$ (line) showing the intermittency of the periodic oscillations.

they are shed in the absence of turbulence. Sufficiently many exchanges between a nascent vortex and any other region in the flow suppress the formation of the vortex, and thus there can be no vortex street. Bearman, in his experimental study on the effects of incident turbulence on flow around flat plates at much higher mean-flow Re ,⁽³⁾ also states that the main effect of turbulence in the incident flow is on the exchange of momentum between flow inside and outside of the wake.

The result that at sufficiently large l_{\max}/D the von Karman street is destroyed is not readily seen by spectral analysis, but is confirmed by an examination of spatial correlation in the flow. Figure 4 shows that the power spectrum of the time series of $v(3.5D, 0)$, $v(w) v^*(w)$, retains a peak near the Strouhal frequency even with $l_{\max} = 7D$, though the velocity oscillations are so small for $l_{\max} \geq 3D$ that they do not seem to be due to translating vortices. To confirm that the persistent peak is not due to vortex shedding, we note that without Lévy exchanges, vortices produce strong spatial correlations in the velocity field which persist far downstream from the obstacle, and that these spatial correlations are feeble and localized for sufficiently large l_{\max}/D . In particular, the quantity $c(x) = \langle \Delta v(x, 0) \Delta v(x, D/2) \rangle$, with $\Delta v(x, y) = v(x, y) - \bar{v}(x, y)$, varies very slowly with x in laminar flow, as may be seen in Fig. 5. This is because vortices retain their coherent structure as they are convected away from the obstacle. For $l_{\max} \geq 3D$, however, the correlation falls off sharply with increasing distance from the obstacle, and is weak even immediately downstream from the obstacle. If the correlation in velocities arose as a consequence of spatially coherent vortices being convected upstream, the correlation should change only as the vortices diffuse away. The transverse velocity does not show such a slowly changing correlation with long exchanges—it is larger in magnitude near the obstacle and shows a stronger spatial correlation there also. Such behavior might be due to oscillation of the vestigial wake. An experimental study⁽¹⁰⁾ performed in turbulent shear flow past a cylinder at lower mean flow Re than Bearman's investigation supports the qualitative conclusion that turbulence with a large integral scale disrupts vortex shedding.

The effect of the momentum exchanges on the velocity field provides a ready interpretation for the changes in the pressure near the obstacle, shown in an inset to Fig. 6. The pressure behind the obstacle is smaller with turbulence than, without, and the pressure in front is larger. The smaller pressure behind the obstacle is a consequence of the weaker backflow in the wake, that is, of the enhanced momentum exchange between the wake and its surroundings. Similarly, exchanges tend to reduce v upstream from the obstacle, thus raising the pressure there. We have checked that the pressure with exchanges shown in the inset to Fig. 6 is insensitive to the form of $N(l)$.

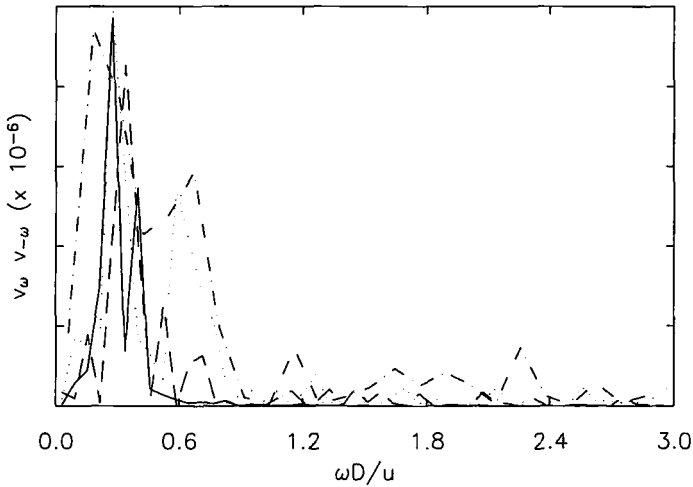


Fig. 4. Power spectra of $v(3.5D, 0)$ for $l_{\max} = 2D$ (solid line), $3D$ (dashed line), $5D$ (dash-dotted line), and $7D$ (dotted line). All curves have been rescaled to have similar maxima.

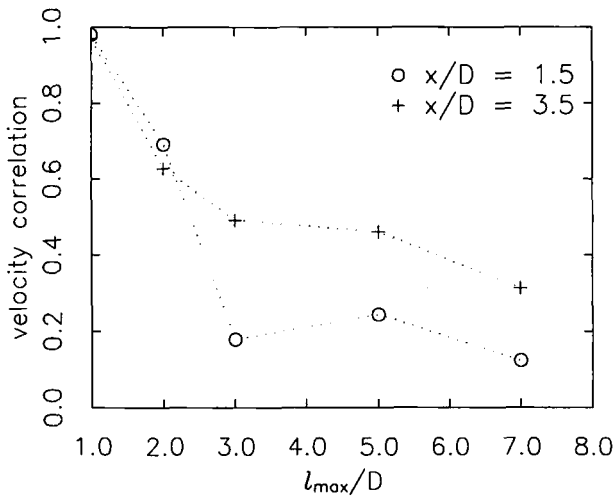


Fig. 5. Correlations in v at two positions downstream from the obstacle. The change from strong correlation weakly dependent on distance from the obstacle to rapidly falling-off weak correlation indicates that the peak near the Strouhal frequency in Fig. 4 is not due to vortex shedding.

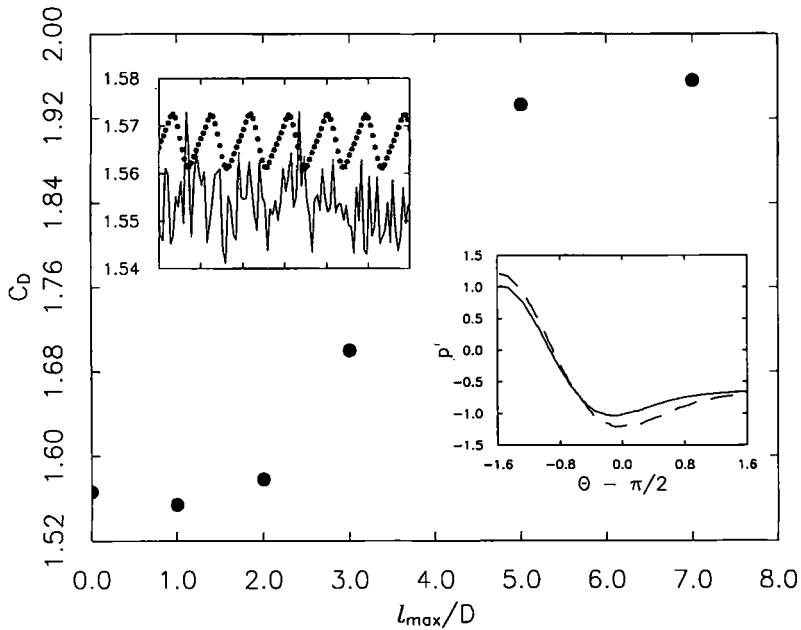


Fig. 6. Drag plotted as a function of l_{\max}/D . The upper inset shows time series of the drag in laminar flow at $Re = 76.8$ and for flow with incident turbulence with $l_{\max} = D$. Even the weakest turbulence, which still leaves the von Karman street intact, is strong enough to mask the small-amplitude oscillations the drag undergoes as vortices are shed. The lower inset is pressure as a function of angle in laminar flow (solid line) and with incident turbulence with $l_{\max} = 7D$ (dash-dotted line).

The drag, shown in Fig. 6 as a function of l_{\max}/D , reflects these changes in the pressure. For small l , the drag reflects the suppression of the vortex street and the enhanced transport of momentum by the Lévy distributed exchanges. Once l_{\max}/D becomes large enough, increasing the size of the largest exchanges is no longer significant, so the change in drag only reflects the slow increase in the probability of long exchanges with further increases in l_{\max} . Exactly how large depends on the choice of $N(l)$. Our results for how turbulence in the incident flow affects pressure and drag are, in qualitative agreement with Bearman's results for flat plates.⁽³⁾

To conclude, we have implemented a Lévy walk-based model for turbulent flow incident on a cylinder (in two dimensions) and found that the regular vortex structure is greatly perturbed by the transport of fluid in and out of the wake when the integral scale of turbulence is large enough

compared to the cylinder diameter. Results on changes in drag and pressure due to incident turbulence are in qualitative agreement with experimental results obtained at very high Reynolds number.

ACKNOWLEDGMENTS

This work was supported by the Department of the Navy, Office of Naval Research, under grant no. N00014-92-J-1271, and benefited from computer time at the Ohio Supercomputer Center.

REFERENCES

1. H. Chen, S. Chen, and W. H. Matthaeus, *Phys. Rev. A* **45**:R5339 (1992).
2. L. Wagner, *Phys. Rev. E* **49**:2115 (1994); *Phys. Fluids* **6**:3516 (1994).
3. P. W. Bearman, *J. Fluid Mech.* **46**:177 (1971).
4. M. F. Schlesinger, B. J. West, and J. Klafter, *Phys. Rev. Lett.* **58**:1100 (1987).
5. F. Hayot and L. Wagner, *Phys. Rev. E* **49**:470 (1994).
6. C. Norberg, in *Bluff-Body Wakes, Dynamics, and Instabilities*, H. Eckelmann, ed. (IUTAM Symposium Series, 1994).
7. A. Roshko, NACA TN-2913 (1953).
8. S. C. R. Dennis and G.-Z. Chang, *J. Fluid Mech.* **42**:471 (1970).
9. S. S. Abarbanel, W. S. Don, D. Gottlieb, D. H. Rudy, and J. Townsend, *J. Fluid Mech.* **225**:557 (1991).
10. M. Kiya and H. Tamura, *J. Fluid Eng.* **111**:126 (1989).